Electronic Supplementary Material (ESI) for CrystEngComm.

Supporting information

Construction of naphthalenediimide-based cadmium complexes and application in iodine adsorption, photochromism and photocatalysis

Ming Yang Sun [a], Feng Ying Bai[a], Qing Lin Guan*[a], Yong Heng Xing [a] and Fen Xu [b]*

[a] College of Chemistry and Chemical Engineering, Liaoning Normal University, Dalian 116029, P. R. China.

[b] Guangxi Key Laboratory of Information Materials, Guilin University of Electronic Technology, Guilin 541004, P. R. China.

E-mail: baifengying2003@163.com (F. Y. Bai); guanqinglin@lnnu.edu.cn (Q. L. Guan)

Contents

Section S1. The synthetics of complexes 1 and 2

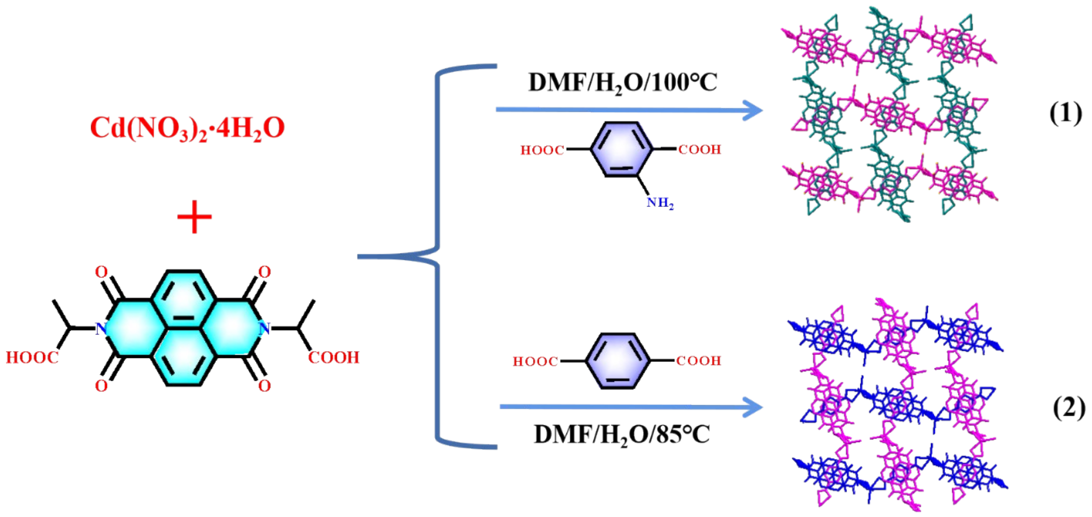

Scheme. S1 The synthetics of complexes **1** and **2**.

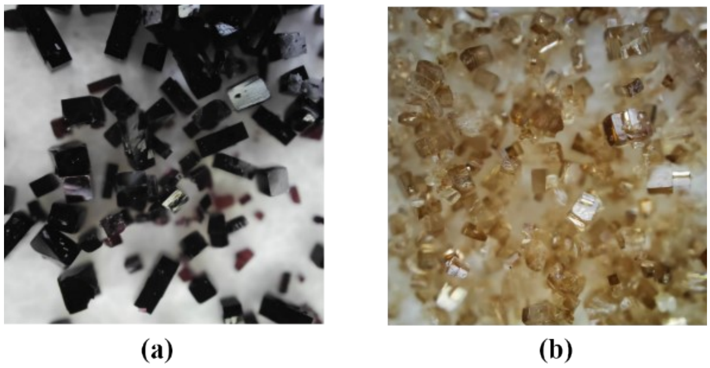

Fig. S1 The crystal image of complexes **1** (a) and **2** (b).

Section S2. Materials and methods

All chemicals commercially were analytical grade or better and purchased and used without further purification. The equipment required for the experiment is in the support information. The maximum absorption wavelength of cyclohexane solution was determined by UV-1000 spectrophotomete (350-800 nm). The Bruker AXS TENSOR-27 FT-IR spectrometer was applied to record infrared spectra in the range of 4000-400 cm^{-1}. UV-vis absorption spectra of solid sample were measured on a JASCO V-570 UV/VIS/NIR spectrophotometer in the range of 200-2500 nm. Thermogravimetric data was obtained on a PerkinElmer Diamond TG/DTA at a 10 °C min^{-1} under nitrogen protection. X-ray powder diffraction (PXRD) patterns were conducted on an Advance D8 equipped with Cu-Kα radiation, in the range of $5° < 2\theta < 50°$, with a step size of 0.02° (2θ) and a count time of 2 s per step.

Section S3. Synthesis of the ligand AlaNDI

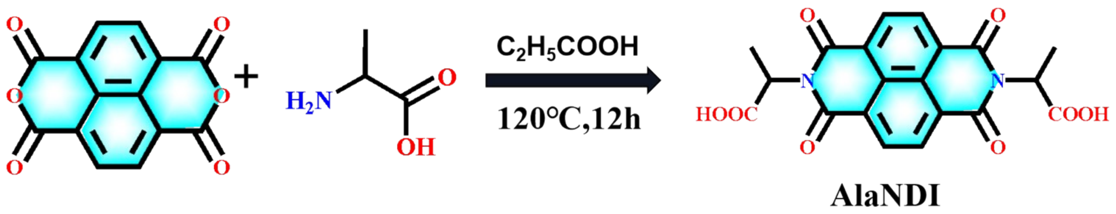

Scheme. S2 Synthesis of the ligand AlaNDI

Ligand AlaNDI was synthesized by modifying the method proposed in literature [1]. A mixture of naphthalene dianhydride (2.68 g, 10 mol) and alanine (1.78 g, 20 mol) were refluxed in 150 mL propionic acid at 120 °C for 12 h. Cool to room temperature, add 50ml distilled water, light yellow precipitation is generated, filtered at atmospheric pressure, wash with anhydrous ethanol, light yellow solid 2.9899 g, the yield is about 74%.

Section S4. The crystalline data of the complexes 1 and 2

Tab. S1 Crystallographic data for complexes **1** and **2***

Empirical formula	**1**	**2**
Formula weight	671.87	703.45
CCDC	2182088	2182066
Crystal system	Orthorhombic	Orthorhombic
Space group	Ibam	Ibam
a/ Å	15.6608(14)	15.7981(13)
b/ Å	16.6690(15)	16.2656(14)
c/ Å	22.238(2)	22.388(2)
α/°	90	90
β/ °	90	90
γ/°	90	90
V/Å^3	5805.3(9)	5753.0(9)
Z	8	8
F (000)	2708.0	1076.0
T/K	296	296
R_{int}	0.0240	0.0637
θ(°)	3.568 - 53.864	3.594 - 56.682
Goodness-of-fit on F^2	1.063	1.079
Reflections collected	16623	7559
Independent reflections	3234	3670
parameters	327	216
R^a	0.0677 (0.2107)^b	0.0868 (0.2542)^b
$wR2^a$	0.0921 (0.2434)^b	0.0868 (0.2542)^b

*Symmetry codes: complex **1**: #1 +x, +y, 1-z. complex **2**: #1 +x, +y, 1-z.

Section S5. IR spectra of complexes 1, 2 and ligands

Tab. S2 Detailed attribute of IR data of ligands and complexes **1** and **2** (cm^{-1})

	AlaNDI	NH_2-BDC	**1**	H_2BDC	**2**
$v_{(N-H)}$	—	3374, 3507	3447, 3338	—	—
$v_{(Ar-H)}$	3076	3070	3076, 3018	3108, 3069	3082
$v_{(C-H)}$	2930, 2880, 2846	—	2945, 2778	—	2938, 2882, 2795
v_{ascoo-}	1746, 1708,	1689	1702, 1663, 1580	1779	1706, 1607, 1579
v_{scoo-}	1458, 1422,	1497,	1492, 1449, 1409	1420	1454, 1407, 1332

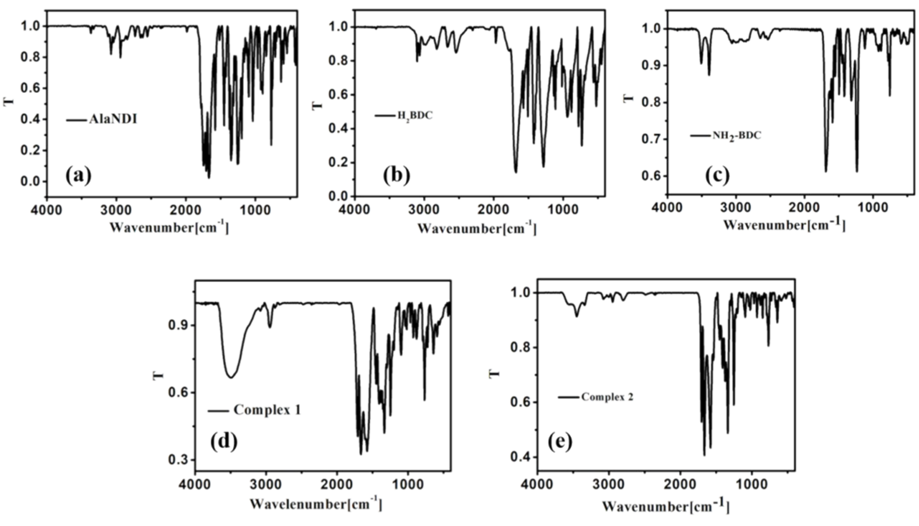

Fig. S2 IR spectra: (a) ligand AlaNDI; (b) ligand H_2BDC; (c) ligand NH_2-H_2BDC; (d) complex **1**; (d) complex **2**.

Section S6. UV-vis characterizations of the complexes 1and 2

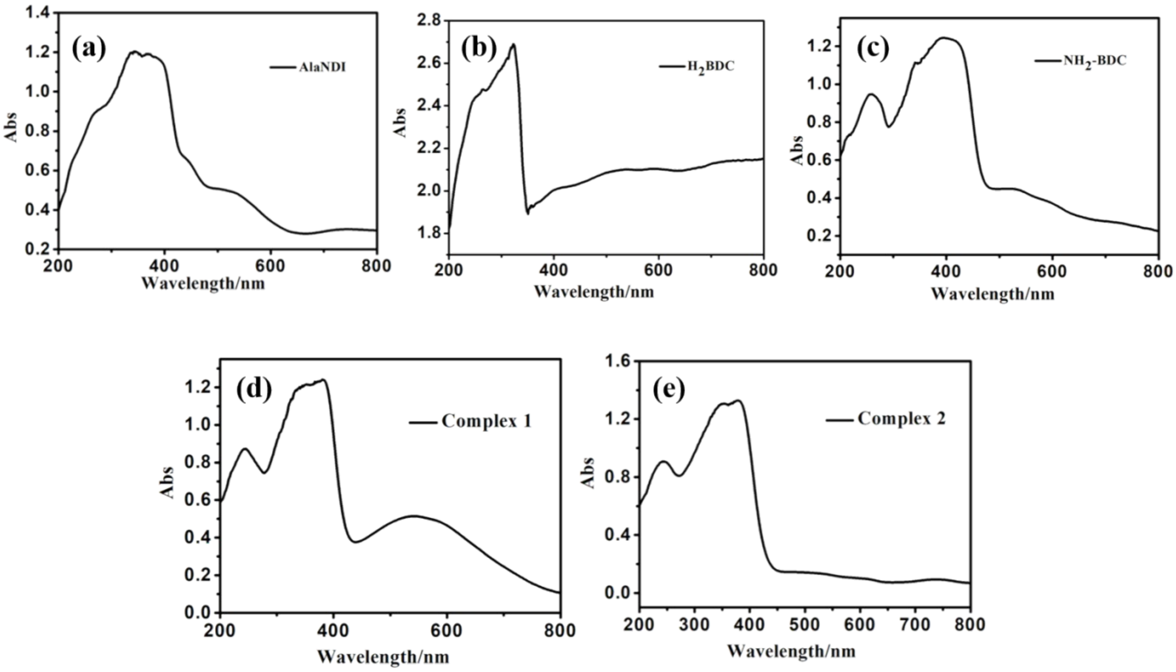

Fig. S3 UV spectra: (a) ligand AlaNDI; (b) ligand H_2BDC; (c) ligand NH_2-H_2BDC; (d) complex **1**; (d) complex **2**.

Tab. S3 UV-vis spectra data (nm) of ligands and complexes **1** and **2**

Complexes	LLCT		ICT
	π-π*	n-π*	
H_2BDC	242	289	
NH_2-H_2BDC	214	250	
AlaNDI	284	370	
1	242	380	547
2	243	379	

Section S7. Fluorescence spectra of complexes 1 and 2

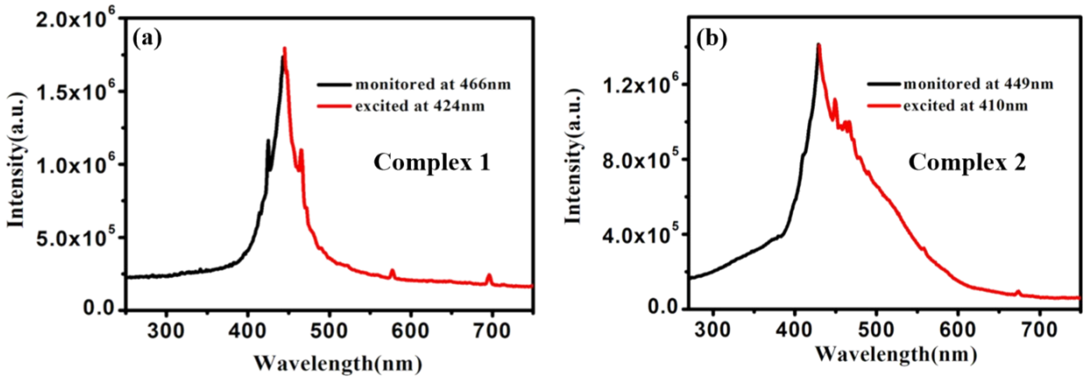

Fig. S4 Excitation and emission spectra of complex **1** (a) and complex **2** (b).

Section S8 Thermal properties of the complexes 1 and 2

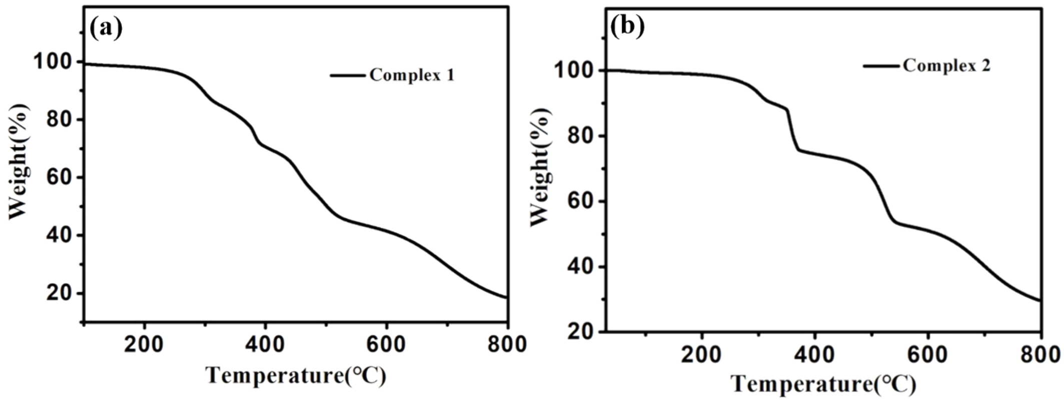

Fig. S5 TG curves of the complex **1** (a) and complex **2** (b).

Section S9 PXRD patterns of the complexes 1 and 2

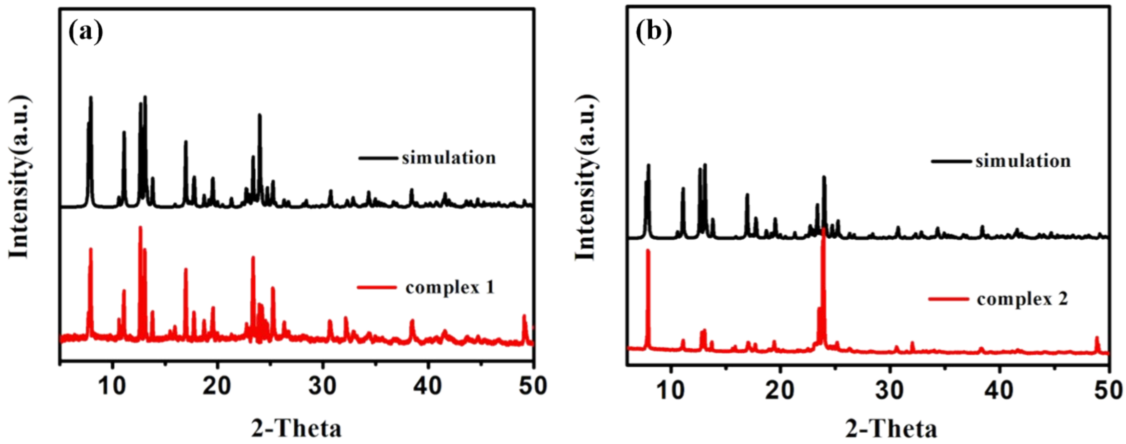

Fig. S6 PXRD patterns of (a) complex **1** and (b) complex **2**.

Section S10. Iodine adsorption Experiments method

Different doses of complexes **1** and **2** were added to iodine cyclohexane solution. It was stirred at room temperature in the dark, and sampled at a fixed time interval, then centrifuged with a centrifuge, at 3000 r/min for 2-3 minutes. The upper clear solution was taken. The maximum absorbance values were monitored by UV-visible spectrophotometer (UV-1000). The change in concentration of iodine solution was calculated by the concentration-absorbance standard curve (Fig. S8), used formula $R = C_0\text{-}C_t/C_0 \times 100\%$ to calculated removal efficiency of iodine for complexes **1** and **2**. Where "C_0" represented the initial concentration ($mg \cdot L^{-1}$) of iodine solution respectively, "C_t" was the concentration of iodine solution at any specific time ($mg \cdot L^{-1}$). Used formula $q_e = [(C_0\text{-}C_e) \times V] / m$ to calculated the maximum adsorption capacity (q_e, mg/g) of iodine for complexes **1** and **2**. Where "C_e" represents the equilibrium concentration after degradation ($mg \cdot L^{-1}$), "V" represented the volume of solution (L), and "m" represented the mass of adsorbent (g).

Section S11. The pseudo-first-order and quasi-second-order kinetic curves of complex 1

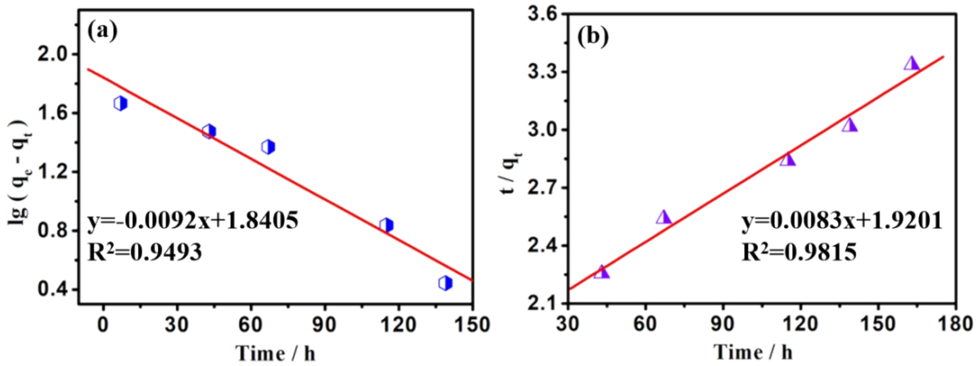

Fig. S7 Plots of the pseudo-first-order (a) and the pseudo-second-order (b) kinetics for the adsorption of I_2 in cyclohexane on complex **1**.

Section S12. Calibration plot of standard iodine in cyclohexane solution

Seven groups of iodine cyclohexane solutions with concentrations of 40, 60, 80, 100, 120, 140, 160 ppm were prepared by dissolving different masses of solid iodine in cyclohexane solution. Firstly, a solution was randomly selected and scanned at full wavelength with UV-visible spectrophotometer (UV-1000). The maximum absorbance was determined by measuring the absorbance values of 6 groups of iodine solutions with different concentrations at the maximum wavelength (λ_{max} = 521 nm), and the absorbance curves with the concentration were obtained (Fig. S8). The standard curve of iodine in cyclohexane solution was obtained by linear fitting of the obtained data (Fig. S8 illustration), and its linear equation was y = 0.0046x-0.0215.

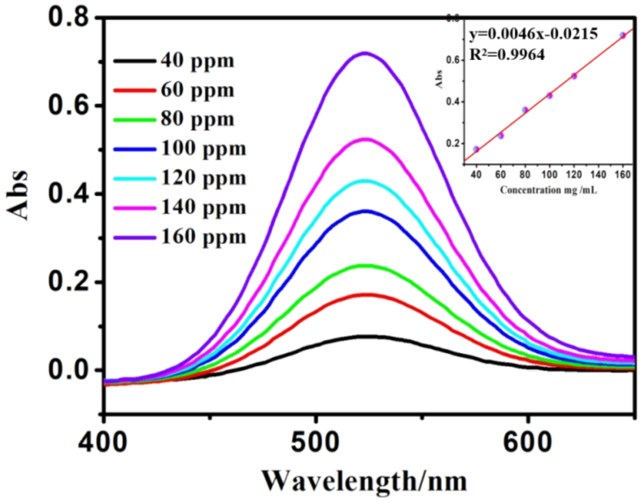

Fig. S8 Calibration plots of standard iodine in cyclohexane solution.

Section S13. Stability of the complex 1 before and after iodine adsorption

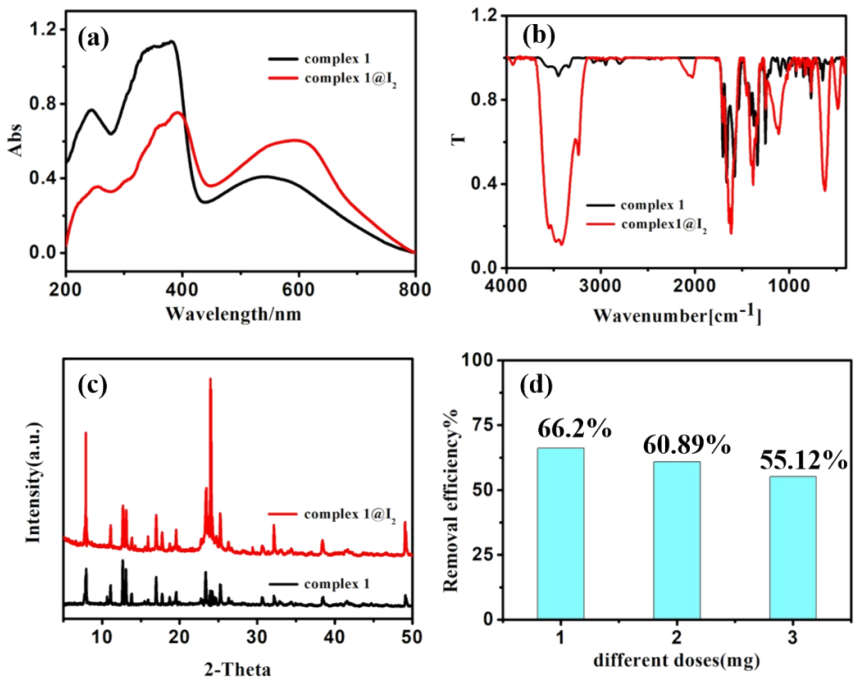

Fig. S9 (a) UV-vis spectra of complex **1** before and after iodine adsorption; (b) IR spectra of complex **1** before and after iodine adsorption; c) PXRD patterns of complex **1** before and after iodine adsorption; (d) Three recycling experiments of iodine adsorption for complex **1**.

Section S14. stability before and after irradiation

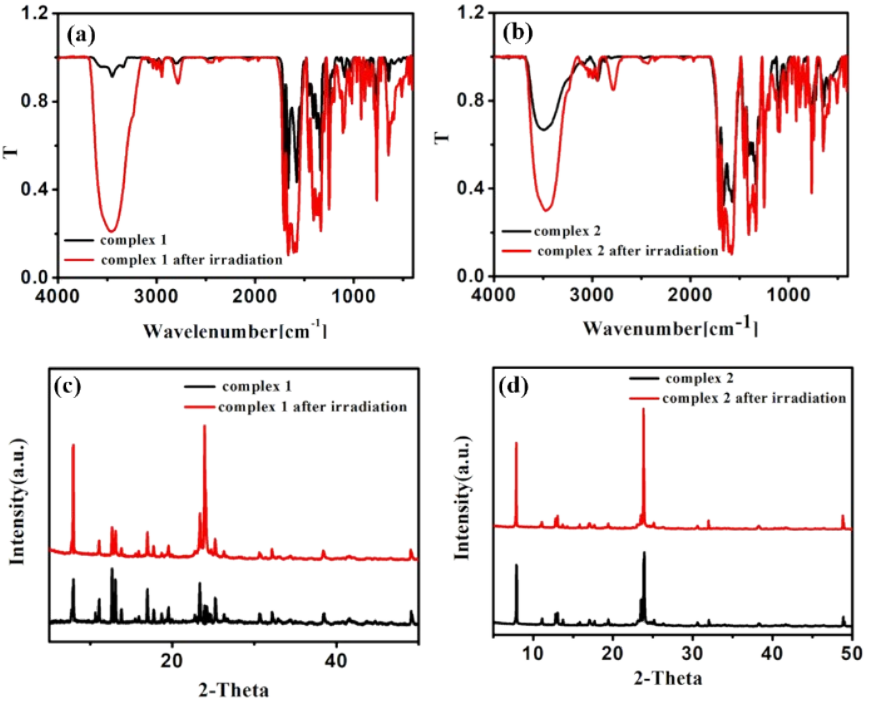

Fig. S10 Comparison of IR spectra before and after irradiation for (a) complex **1** (b) complex **2**; Comparison of PXRD patterns before and after irradiation for (c) complex **1** (d) complex **2**.

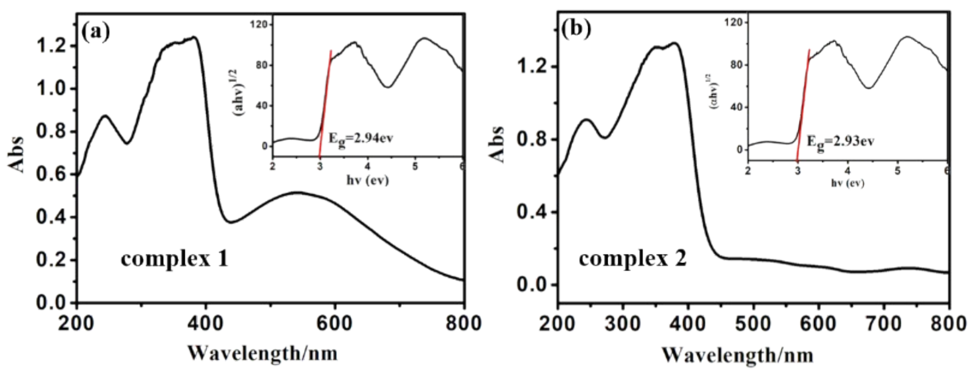

Section S15. Band gap values of the complexes 1 and 2

Fig. S11 Band gap values of the complexes **1** and **2**.

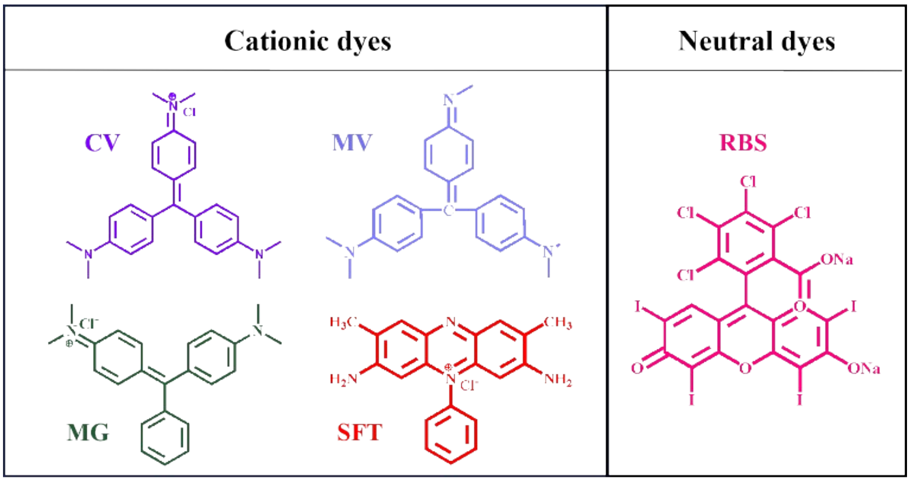

Section S16. Structures of different dyes

Fig. S12 Structures of different dyes for degradation.

Section S17. Photocatalytic dye degradation

Fig. S13 Time dependent UV scan curves for photodegradation of the dye CV at room

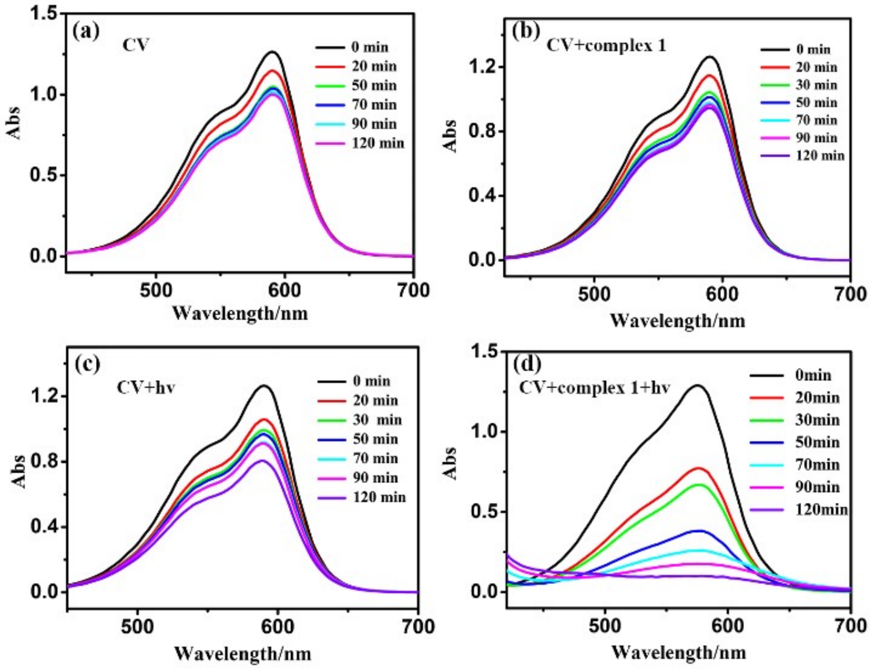

temperature: (a) CV; (b) CV + complex 1; (c) CV + hv; (d) CV+ complex 1 +hv.

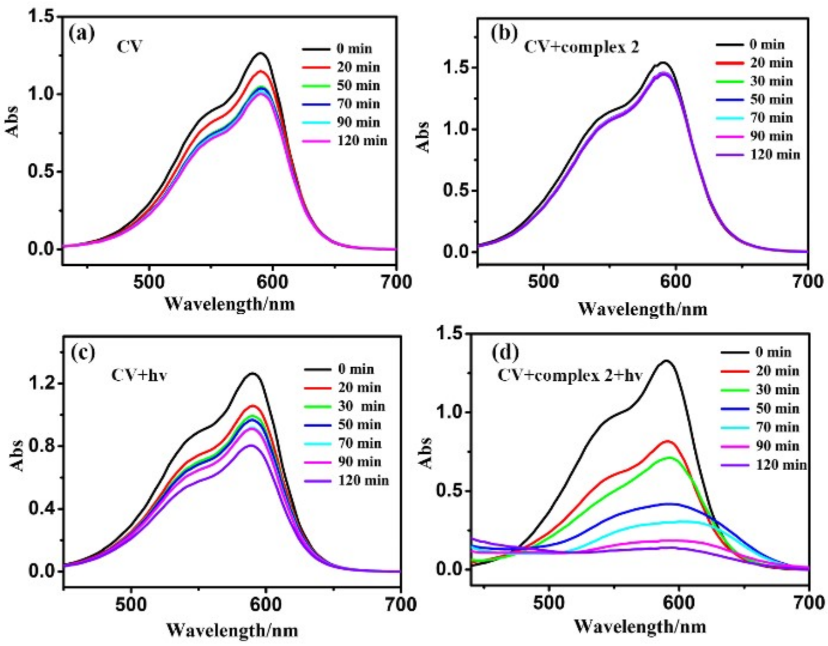

Fig.S14 Time dependent UV scan curves for photodegradation of the dye CV at room temperature: (a) CV; (b) CV + complex 2; (c) CV+hv; (d) CV+complex 2 +hv.

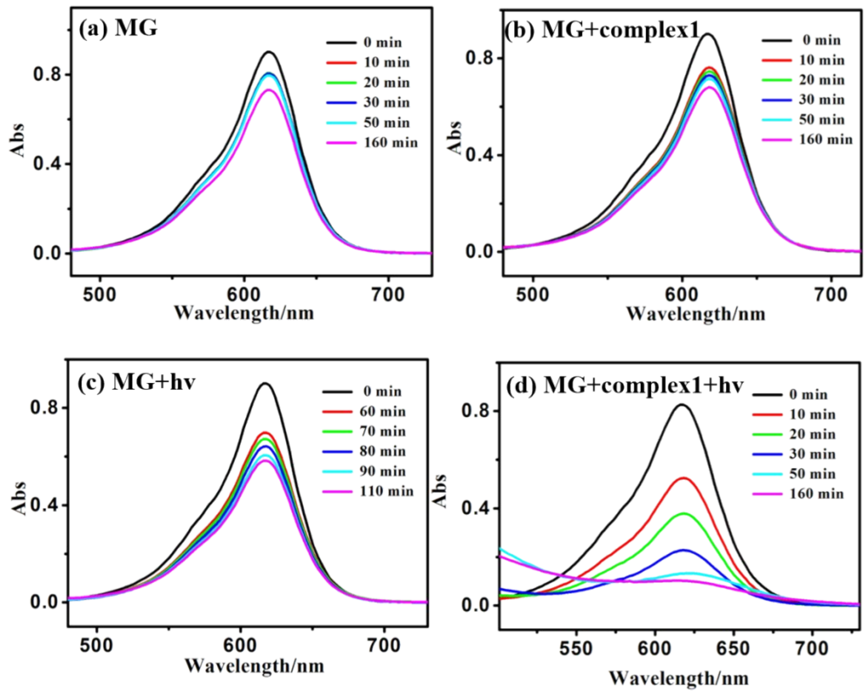

Fig. S15 Time dependent UV-vis spectra for photodegradation at room temperature: (a) MG; (b) MG + complex **1**; (c) MG +hv; (d) MG +complex **1** +hv.

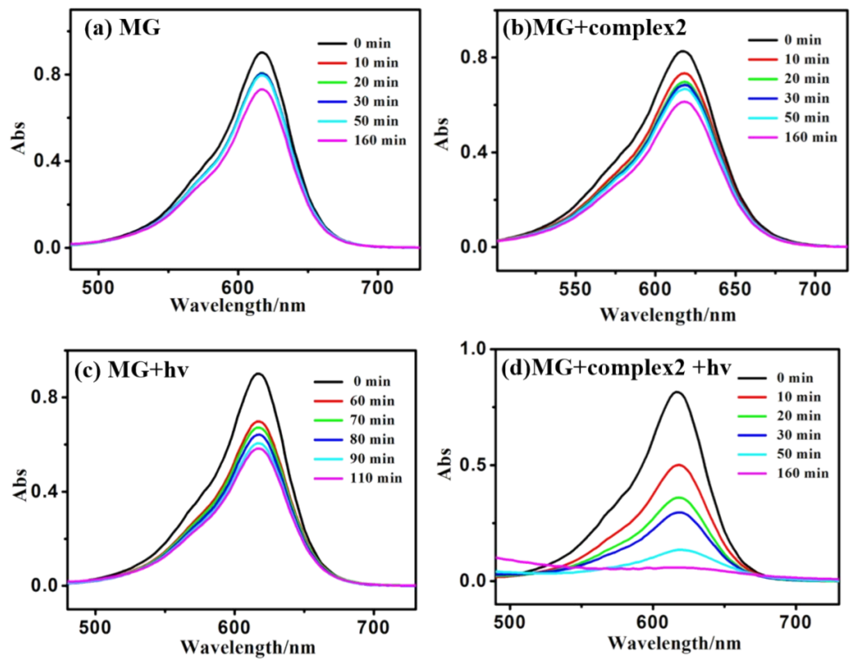

Fig. S16 Time dependent UV-vis spectra for photodegradation at room temperature: (a) MG; (b) MG + complex **2**; (c) MG +hv; (d) MG +complex **2** +hv.

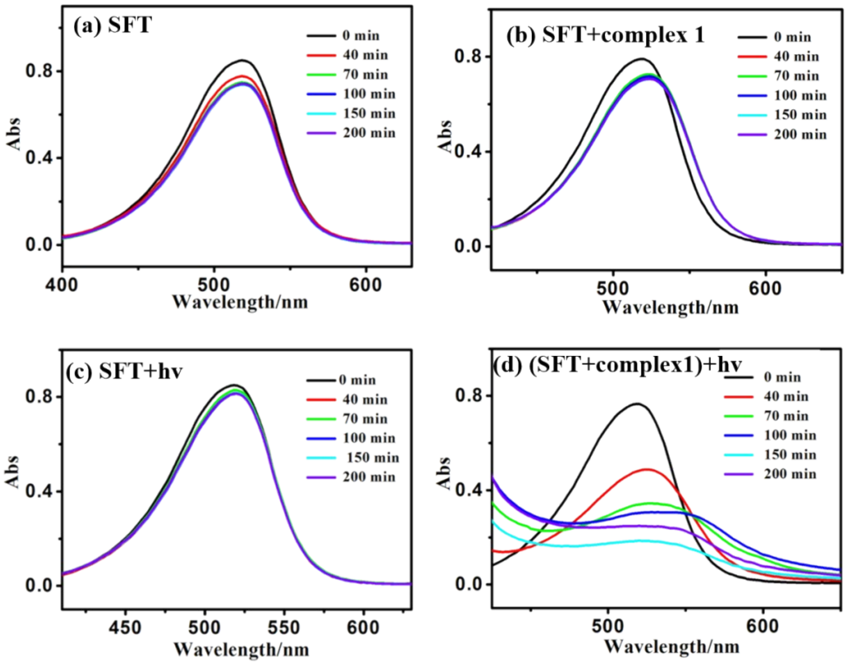

Fig. S17 Time dependent UV-vis spectra for photodegradation at room temperature: (a) SFT; (b) SFT + complex **1**; (c) SFT +hv; (d) SFT +complex **1** +hv.

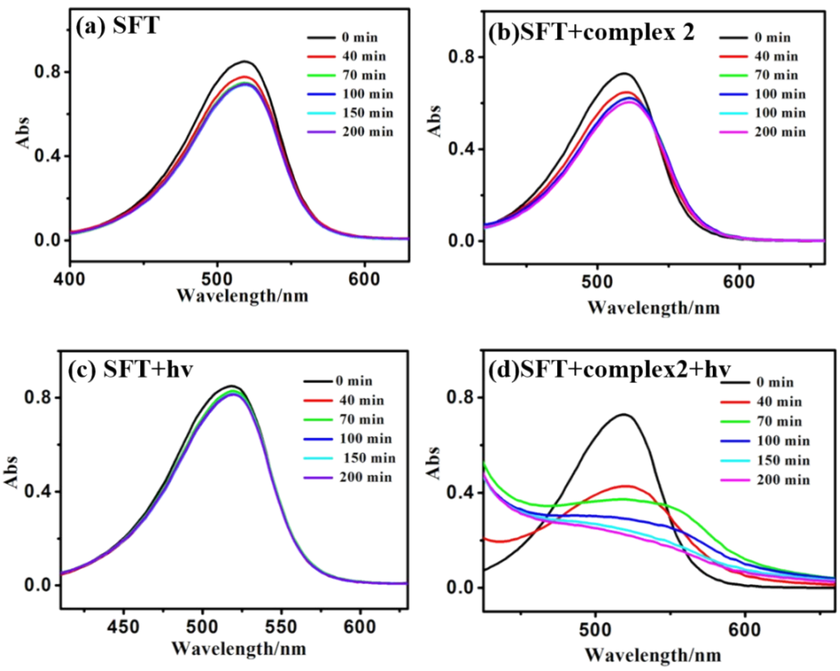

Fig. S18 Time dependent UV-vis spectra for photodegradation at room temperature: (a) SFT; (b) SFT + complex **2**; (c) SFT +hv; (d) SFT +complex **2** +hv.

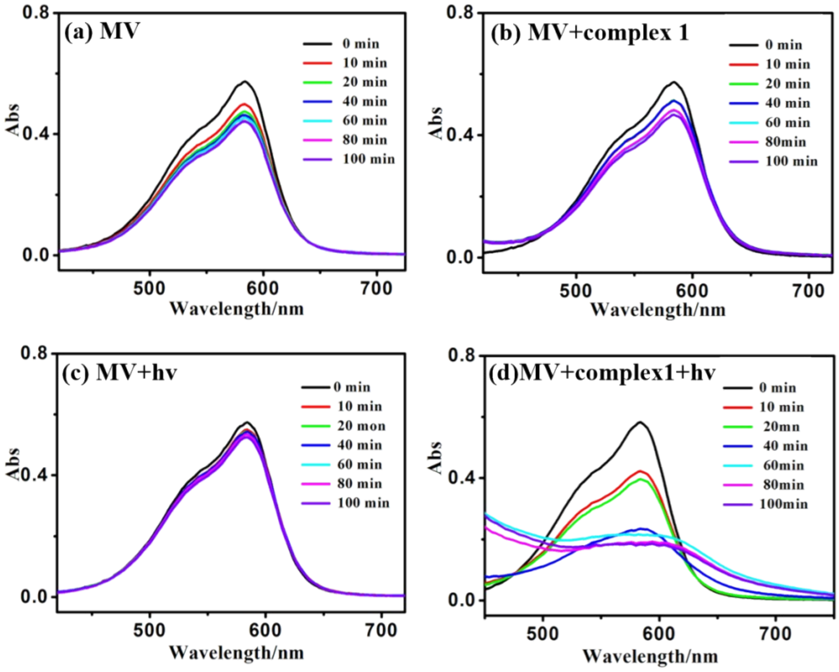

Fig. S19 Time dependent UV-vis spectra for photodegradation at room temperature: (a) MV; (b) MV + complex **1**; (c) MV +hv; (d) MV +complex **1** + hv.

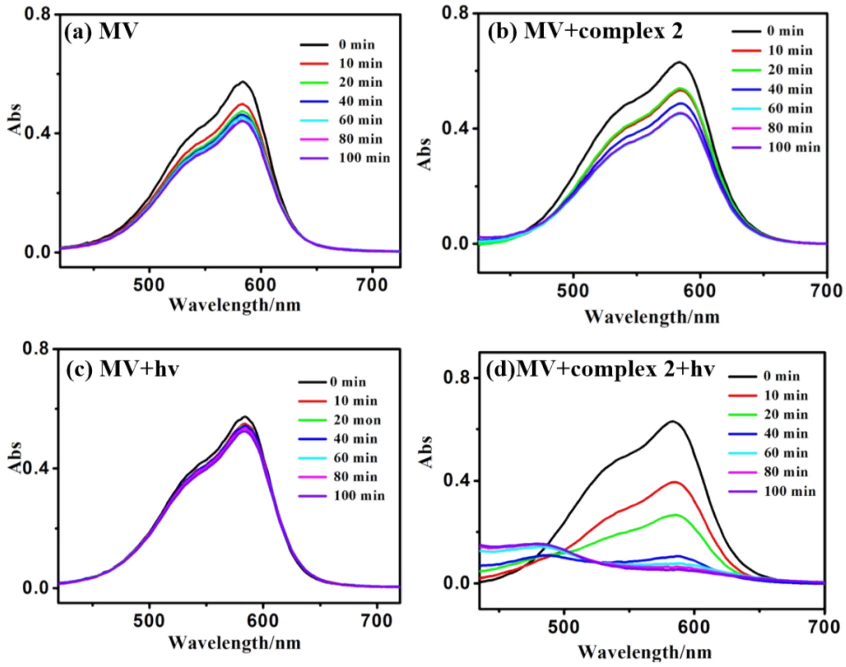

Fig. S20 Time dependent UV-vis spectra for photodegradation at room temperature: (a) MV; (b) MV + complex **2**; (c) MV +hv; (d) MV +complex **2** +hv.

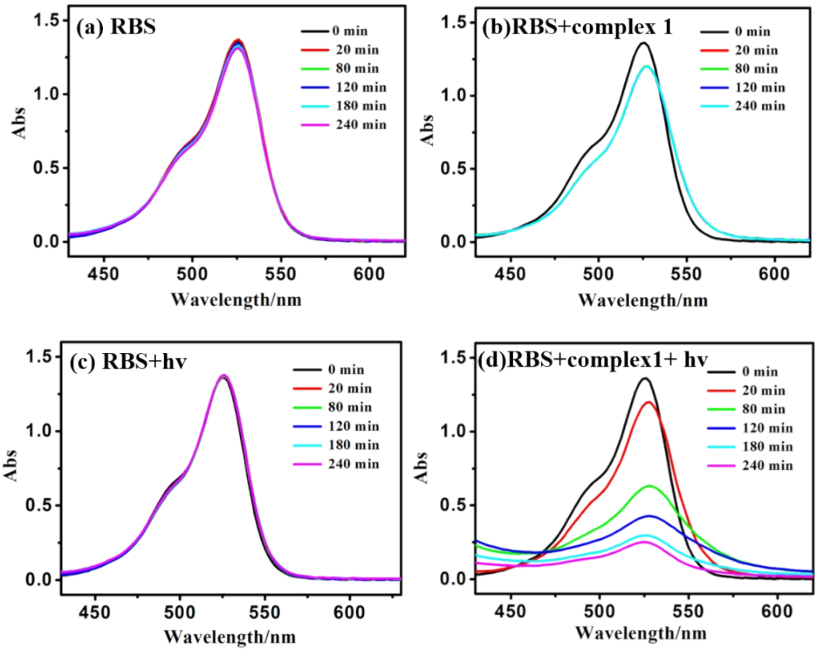

Fig. S21 Time dependent UV-vis spectra for photodegradation at room temperature: (a) RBS; (b) RBS + complex **1**; (c) RBS +hv; (d) RBS +complex **1** +hv.

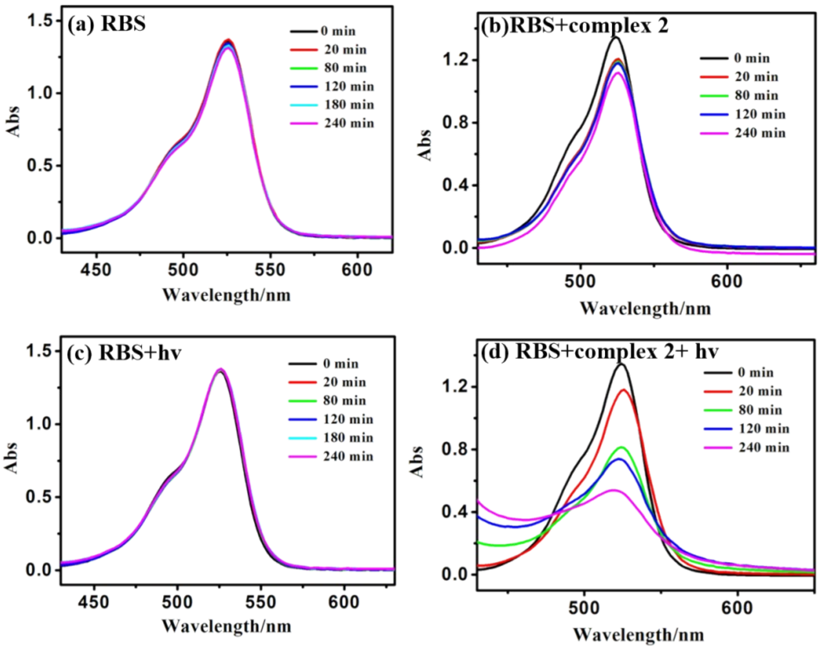

Fig. S22 Time dependent UV-vis spectra for photodegradation at room temperature: (a) RBS; (b) RBS + complex **2**; (c) RBS +hv; (d) RBS +complex **2** +hv.

Section S18. Different doses of the complex 1 for photodegradation and quasi first-order kinetics curves of the dye CV

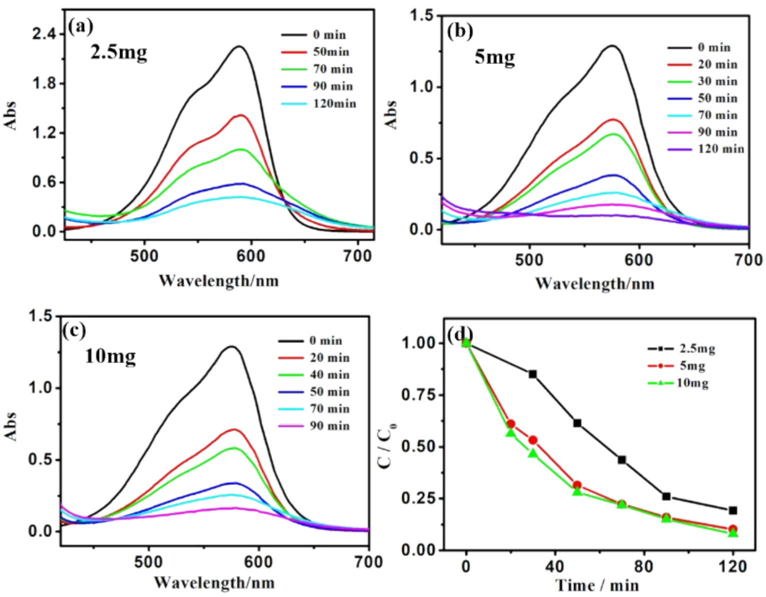

Fig. S23 Time dependent UV-vis spectra for photodegradation of the dye CV with complex **1** at room temperature (a) 2.5 mg; (b) 5 mg; (c) 10 mg. (d) Comparison of C/C_0 with different catalyst doses.

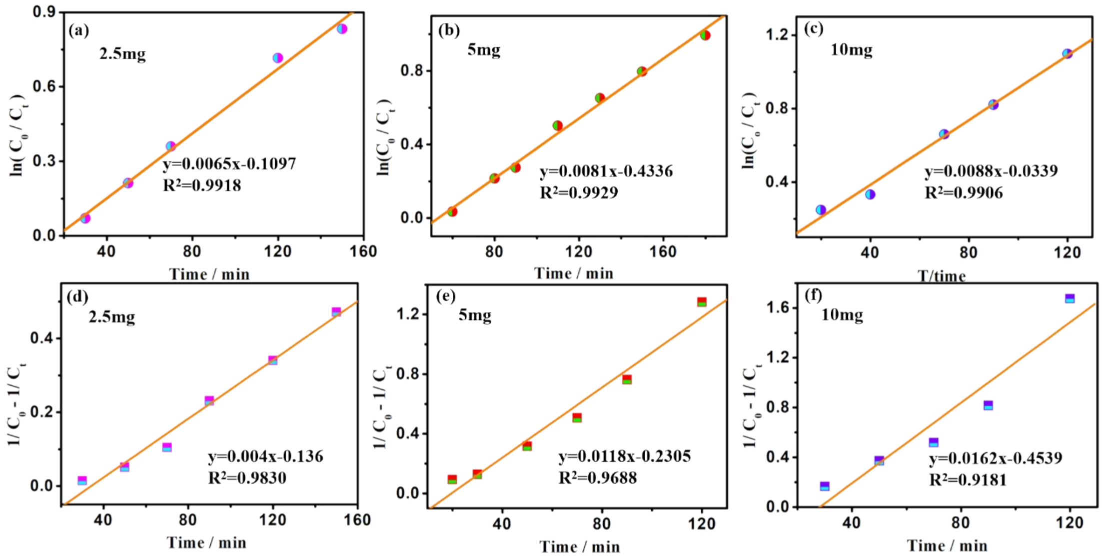

Fig. S24 The different does of quasi first-order kinetics curves of CV dye for complex **1**; (a) 2.5mg; (b)5mg; (c) 10mg; The different does of quasi second-order kinetics curves of CV dye for complex **1** (d) 2.5mg; (e)5mg; (f) 10mg.

Section S19.   Kinetic analysis

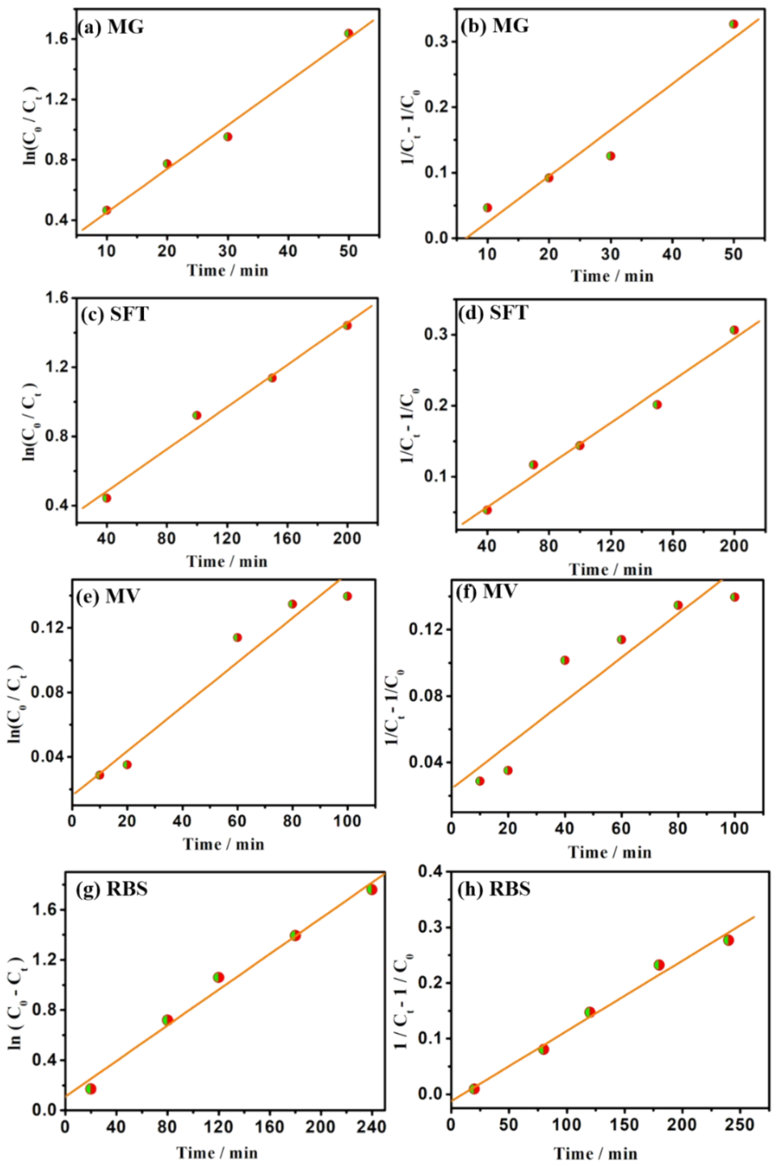

Fig. S25 The quasi first-order and second-order kinetics curves of different dye for complex **1**; (a) (b) MG dye; (c) (d) SFT dye; (e) (f) MV dye; (f) (g) RBS dye.

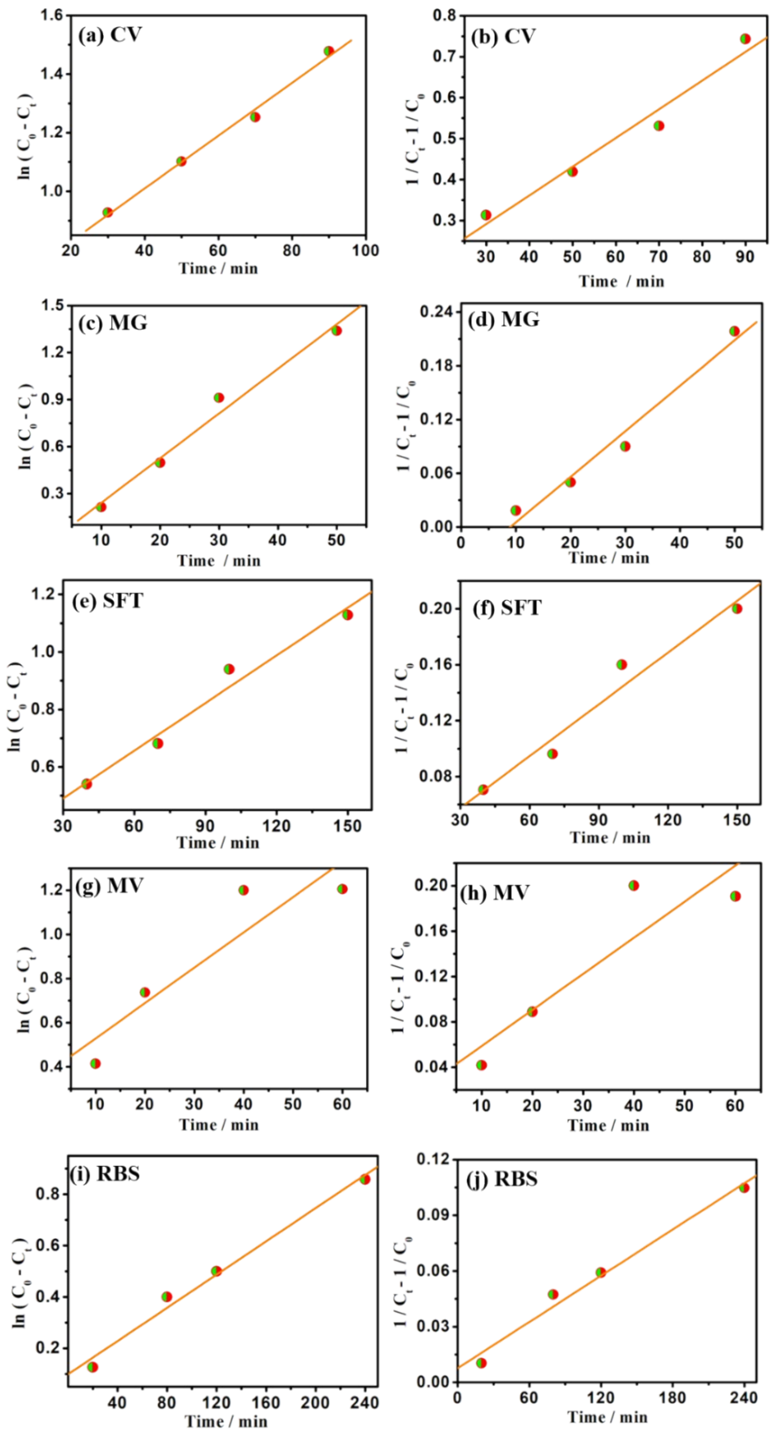

Fig. S26 The quasi first-order and second-order kinetics curves of different dye for complex **2**; (a) (b) CV dye; (c) (d) MG dye; (e) (f) SFT dye; (f) (g) MV dye; (i) (j) RBS dye.

Section S20. Recycling experiments for the photocatalytic degradation of CV by complex 1

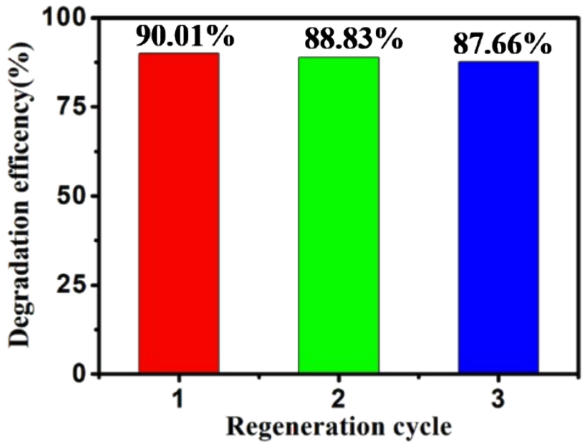

Fig. S27 Three Recycling experiments for the photocatalytic degradation of CV by complex **1**.

Section S21. Mechanism of photocatalytic degradation of dyes

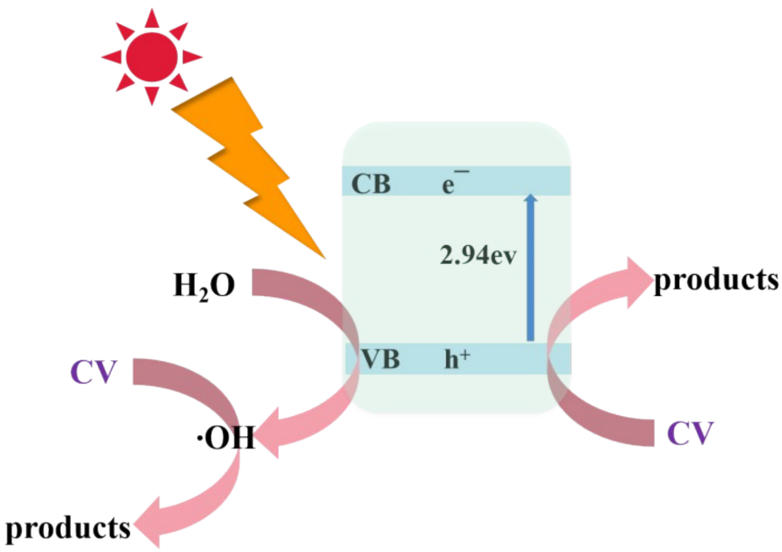

Fig. 28 Mechanism diagram of photocatalytic degradation of dyes.

References

[1] X. B. Shang, I. Song, J. H. Lee, W. Choi, H. Ohtsu, G. Y. Jung, J. Ahn, M. Han, J. Y. Koo, M. Kawano, S. K. Kwak, J. H. Oh, ACS Applied Materials & Interfaces, 2019, **11**, 20174-20182.